Relationship between markers of disease activity and progression in skeletal muscle of GNE myopathy patients using quantitative nuclear magnetic resonance imaging and ^{31}P nuclear magnetic resonance spectroscopy

Harmen Reyngoudt[1,2], Benjamin Marty[1,2], Ericky Caldas de Almeida Araújo[1,2], Pierre-Yves Baudin[3], Julien Le Louër[1,2], Jean-Marc Boisserie[1,2], Anthony Béhin[4], Laurent Servais[5,6,7,8], Teresa Gidaro[5,6], Pierre G. Carlier[1,2]

[1]NMR Laboratory, Neuromuscular Investigation Center, Institute of Myology, Paris, France; [2]NMR Laboratory, CEA, DRF, IBFJ, MIRCen, Paris, France; [3]Consultants for Research in Imaging and Spectroscopy (C.R.I.S.), Tournai, Belgium; [4]Neuromuscular Reference Center, Institute of Myology, Pitié-Salpêtrière Hospital (AP-HP), Paris, France; [5]Institute of Myology, Pitié-Salpêtrière Hospital (AP-HP), Paris, France; [6]I-Motion–Pediatric Clinical Trials Department, Trousseau Hospital (AP-HP), Paris, France; [7]Centre de référence des maladies Neuromusculaires, CHU, University of Liège, Liège, Belgium; [8]MDUK Oxford Neuromuscular Center, Department of Pediatrics, University of Oxford, Oxford, UK

Correspondence to: Harmen Reyngoudt, PhD. NMR Laboratory, Neuromuscular Investigation Center, Institute of Myology, Bâtiment Babinski, Groupe Hospitalier Pitié-Salpêtrière, 47-83 boulevard Vincent Auriol, 75651, Paris Cedex 13, France. Email: h.reyngoudt@institut-myologie.org.

Background: Quantitative nuclear magnetic resonance imaging (NMRI) is an objective and precise outcome measure for evaluating disease progression in neuromuscular disorders. We aimed to investigate predictive 'disease activity' NMR indices, including water T_2 and ^{31}P NMR spectroscopy (NMRS), and its relation to NMR markers of 'disease progression', such as the changes in fat fraction (ΔFat%) and contractile cross-sectional area (ΔcCSA), in GNE myopathy (GNEM) patients.

Methods: NMR was performed on a 3T clinical scanner, at baseline and at a 1-year interval, in 10 GNEM patients and 29 age-matched controls. Dixon-based fat-water imaging and water T_2 mapping were acquired in legs and thighs, and in the dominant forearm. ^{31}P NMRS was performed at the level of quadriceps and hamstring. Water T_2 and ^{31}P NMRS indices were determined for all muscle groups and visits. Correlations were performed with 'disease progression' indices ΔFat%, ΔcCSA and the muscle fat transformation rate (R_{muscle_transf}).

Results: In quadriceps, known to be relatively preserved in GNEM, water T_2 at baseline was significantly higher compared to controls, and correlated strongly with the one-year evolution of Fat% and cCSA and R_{muscle_transf}. Various ^{31}P NMRS indices showed significant differences in quadriceps and hamstring compared to controls and correlations existed between these indices and ΔFat%, ΔcCSA and R_{muscle_transf}.

Conclusions: This study demonstrates that disease activity indices such as water T_2 and ^{31}P NMRS may predict disease progression in skeletal muscles of GNEM patients, and suggests that these measures may be considered to be valuable surrogate endpoints in the assessment of GNEM disease progression.

Keywords: GNE myopathy (GNEM); quantitative nuclear magnetic resonance imaging (quantitative NMRI); ^{31}P nuclear magnetic resonance spectroscopy (^{31}P NMRS); water T_2; skeletal muscle

Introduction

GNE myopathy (GNEM) is a rare, autosomal recessive, progressive neuromuscular disorder, caused by mutations in the UDP-N-acetylglucosamine 2-epimerase/N-acetylmannosamine kinase gene (abbreviated as *GNE*), which is a bifunctional enzyme of the sialic acid biosynthetic pathway (1). Sialic acids play an important role in maintaining membrane stability (2), and a decrease in sialic acid production will result in a reduced sialylation, which is the incorporation of sialic acid in glycoproteins and glycolipids, found in large numbers in cellular membranes (3). Reduced levels of sialic acid were observed in a mouse model expressing mutated *GNE* (4) that develop a pathology resembling a rimmed vacuolar myopathy (4) and named after the autophagic byproducts called 'rimmed vacuoles' (5). The exact mechanisms leading to these aggregates are still unknown. Although some degree of inflammation is a common feature in (sporadic) inclusion body myositis (3), it is usually not observed in GNEM. GNEM is characterized by an onset typically in the third decade of life, with initial distal lower limb muscle atrophy as a clinical presentation and a gradual spreading to more proximal muscles and upper limb (5).

Qualitative T_1-weighted nuclear magnetic resonance imaging (NMRI) revealed fatty infiltrations in all leg (6), thigh (6,7), gluteus (6,8) and forearm (9) muscles. The disorder is known for the relative preservation of the quadriceps (QUAD), yet affected by fatty replacement in the later stages of the disease (3). Currently, quantitative NMRI is being used more and more in the evaluation of the disease of neuromuscular disorders (10) such as Duchenne muscular dystrophy (DMD) (11-13), Becker muscular dystrophy (BMD) (14), facioscapulohumeral muscular dystrophy (FSHD) (15), limb-girdle muscular dystrophy type 2I (16), late-onset Pompe disease (17) and inclusion body myositis (18). Most of these quantitative NMRI studies included a muscle-to-muscle-based determination of fat fraction (Fat%), often derived from Dixon-based water-fat separation approaches, and used as an outcome measure for disease progression. In a recent publication, we have reported significant changes in disease progression (i.e., change in Fat% and contractile cross-sectional area or cCSA) that were detected over the course of one year in GNEM patients using water-fat separation-based quantitative NMRI, whereas functional and strength tests could not demonstrate this progression (19).

Other NMR parameters such as muscle water T_2 and phosphorus (^{31}P) NMR spectroscopy (NMRS) indices have also been investigated in neuromuscular disorders, although to a lesser extent (11,12,14,17,20). These NMR biomarkers may, in fact, indicate abnormalities related to the underlying pathophysiological mechanisms, and could, therefore, be observed as markers of 'disease activity' (10). Specifically, in the case of T_2, using qualitative T_2-weighted NMR images, hyperintensities have been observed in the tibialis anterior and the medio-posterior part of the thigh in GNEM patients (6,9). This qualitative approach used in diagnostic imaging, not in the least in inflammatory myopathies (21-26), is based on visual evaluation of contrast differences between normal and abnormal muscle tissue. Besides the subjective nature of visual scoring of the T_2-weighted approach, patients showing systemic inflammation across all investigated muscles might be erroneously categorized as false negatives (26). Quantitative muscle water T_2, however, cancel out these aforementioned limitations of T_2-weighted NMRI. Due to the sensitivity of water T_2 to changes in muscle composition, it has been proposed as a quantitative outcome measure in a number of neuromuscular disorders, including late-onset Pompe disease (17), DMD (12,20,27) and inflammatory myopathies such as dermatomyositis (28) and inclusion body myositis (18,29). A study in healthy volunteers has also illustrated changes in water T_2 values with ageing (30). Quantitative water T_2 evaluations allow to mutually compare patients and/or to assess the changes within patients in longitudinal studies.

The purpose of the current work was to assess changes of water T_2 and ^{31}P NMRS indices in a one-year longitudinal study of GNEM patients. We investigated the predictive value of these 'disease activity' indices, by determining their relationship with parameters reflecting the disease progression (i.e., change in Fat% and cCSA), and, hence, to assess whether these indices prove to constitute surrogate endpoints in the longitudinal evaluation of GNEM.

Methods

Study population

The NMR protocol was performed at baseline and at a 1-year interval in 10 GNEM patients (mean age, 47±15 years; range, 25–73 years; 5 male, 3 non-ambulant), as previously described (19), and 29 age-matched healthy control subjects (mean age, 48±14 years; range, 18–70 years; 17 male). The patients were included from the French cohort of the Ultragenyx GNE-Myopathy Disease

1452

Reyngoudt et al. Water T_2 NMRI and ^{31}P NMRS in skeletal muscle in GNE myopathy

Monitoring Program (GNEM-DMP UX001-CL401), participating in the ClinBio GNE study. GNEM diagnosis was genetically confirmed. Healthy control subjects were scanned as part of a methodology NMRI/S protocol approved by the local ethics committee (CPP-Ile de France VI–Groupe Hospitalier Pitié-Salpêtrière, ID RCB: 2012-A01689-34) and informed consent was obtained from all controls and patients.

NMR acquisitions

NMR data were acquired on a 3-T clinical system (Trio until December 2014 or PrismaFit from January 2015, Siemens Healthineers, Erlangen, Germany). For quantitative NMRI, the system's body coil for radiofrequency transmission was used with two 18-channel phase array surface coils (Siemens) covering both legs and thighs or a 4-phase array surface coil (Siemens) covering the dominant forearm, combined with a 32-channel spine coil (Siemens) for signal collection. Additionally, for ^{31}P NMRS experiments, a dual-tuned ^{31}P/^{1}H transmit/receive surface coil (RAPID Biomedical GmbH, Rimpar, Germany) was placed over the thigh (centered at mid-femur), once on the anterior side, once on the posterior side, interrogating the QUAD and the hamstring (HSTR) muscles, respectively. We have described subject position in detail in a recently published work (19).

The NMR protocol began with a whole-body (3-point) Dixon acquisition (i.e., multiple 3D gradient echo sequences for quantitative water-fat imaging across the entire body), employing a methodology described in an earlier publication by some of the co-authors of this work (31). The objective of the whole-body Dixon measurement was to determine which of the segments demonstrated an overall Fat% >60%, which was determined as the upper limit for performing further quantitative NMRI and ^{31}P NMRS.

Indeed, the actual quantitative NMRI protocol in this study comprised the acquisition of 3-point Dixon and water T_2 mapping NMRI sequences at the level of the legs, the thighs and the domination forearm, separately. Details of the 3-point Dixon NMRI sequence were described in a separate publication in GNEM (19). For water T_2 mapping, a multi-slice multi-echo (MSME) sequence was employed, covering 3 slices in the forearm and 9 slices in legs and thighs (10 mm slice thickness) and the following acquisition parameters: a train of 17 equidistant echoes (8.7 to 147.9 ms for the forearm; 9.5 to 161.5 ms for the legs/thighs); TR = 4,000 ms (forearm) or 3,000 ms (legs/thighs); nominal

flip angles = 90° and 180°; field-of-view = 104×128 mm^2 (forearm) or 224×448 mm^2 (legs/thighs); spatial resolution = 1×1 mm^2 (forearm) or 1.4×1.4 mm^2 (legs/thighs); bandwidth = 445 Hz/pixel; slice gap = 30 mm; acquisition time = 5 min 18 s (forearm) or 3 min 45 s (legs/thighs). For calculating the transmit field (B$_1^+$) spatial distribution, the XFL sequence (32), which is a fast gradient echo image, was run covering the same volume as the MSME sequence, with the following parameters: TR = 2,000 ms (forearm) or 4,750 ms (legs/thighs); TE = 1.78 ms, flip angle = 8°.

^{31}P NMRS data were obtained from a non-localized 500-µs hard pulse excitation with a TR of 4,000 ms, 64 averages, a bandwidth of 3,000 Hz, 2,048 data points, and an acquisition time of 4 min 16 s. For additional details about the ^{31}P NMRS acquisitions, we refer to earlier publications (11,20).

NMR processing

All quantitative NMRI data were processed using in-house written code. Regions of interest (ROIs) were drawn manually, by the same operator, both on the out-of-phase Dixon and the MSME images, using a free software tool (www.itksnap.org). The ROIs were drawn on both left and right side, except for the forearm where only the dominant side was assessed. For the determination of Fat% and CSA, ROIs were drawn, respectively on the Dixon and the MSME images, in different muscle groups and therefore including intermuscular fat: the QUAD muscle group (comprising vastus lateralis, vastus medialis, vastus intermedius and rectus femoris muscles) and the HSTR muscle group (comprising biceps femoris, semimembranosus and semitendinosus muscles) of the thigh; the triceps surae (TRIC) muscle group (comprising soleus, gastrocnemius medialis and gastrocnemius lateralis muscles), the fibularis (FIB) muscle group and the extensor (EXT_LEG) muscle group (comprising tibialis anterior and extensor digitorum muscles) of the leg; and the flexor (FLEX) muscle group (comprising flexor carpi radialis, flexor carpi ulnaris, flexor digitorum profundus and flexor digitorum superficialis muscles) and the extensor (EXT_FOREARM) muscle group (comprising extensor pollicis longus, extensor carpi radialis, extensor carpi ulnaris, extensor digiti minimi and extensor digitorum muscles) of the forearm.

Using the Dixon images, Fat% values (expressed in percentage) were computed as the ratio between the fat signal and the sum of the water and fat signals. The Fat% value per muscle group was determined as a weighted

average across five central slices (corresponding to the five central slices acquired with MSME, see further on in the text). The values for CSA were calculated in the same muscle groups on the same slices on the co-registered MSME images. The CSA value per muscle group was a mean value across these slices. The contractile CSA (cCSA), defined as the lean muscle CSA corresponding to the muscle volume fraction containing the contractile apparatus, was determined as follows:

$$cCSA = CSA \cdot \left[1 - (0.01 \cdot Fat\%) \right] \qquad [1]$$

Indices of disease progression were the Fat% change after 1 year ($\Delta Fat\%$, in %), the muscle transformation rate (R_{muscle_transf}, in year^{-1}), the (absolute) change in cCSA ($\Delta cCSA$, in mm^2), and the relative change in cCSA ($\Delta cCSA_{rel}$, in %); and were calculated as follows (with baseline and year-1 abbreviated as BL and Y1):

$$\Delta Fat\% = Fat\%_{Y1} - Fat\%_{BL} \qquad [2]$$

$$R_{muscle\_transf} = \frac{\Delta Fat\%}{100 - Fat\%_{BL}} \qquad [3]$$

$$\Delta cCSA = cCSA_{Y1} - cCSA_{BL} \qquad [4]$$

$$\Delta cCSA_{rel} = \frac{cCSA_{Y1} - cCSA_{BL}}{cCSA_{BL}} \cdot 100 \qquad [5]$$

For assessment of water T_2, ROIs delineated the interior of the muscle avoiding fasciae and blood vessels (33). ROIs for water T_2 were drawn FIB, in the individual muscles of EXT_LEG, TRIC, QUAD and HSTR, as well as in the muscle groups EXT_FOREARM and FLEX (because of the difficulty to distinguish the different muscles in these groups). The MSME images were processed based on a tri-exponential fitting procedure (33), which is a model that takes into account both water and fat components in the muscle tissue. Water T_2 values were determined as a mean value within the drawn muscle ROIs, averaged across the five centrally acquired slices (*Figure 1*). The acquisition of a B_1 map enabled voxel sorting by eliminating those voxels having a B_1^+-value outside the prescribed boundaries (i.e., lower than 80% or higher than 120% of the nominal flip angle). The threshold for abnormal water T_2 was set at two standard deviations above mean muscle water T_2 in healthy volunteers, which is approximately 39 ms on the system used in this work (33). Water T_2 values of individual muscles were pooled, weighted by the size of the ROI, to compare with all other measured NMR indices which were all determined on a muscle group level.

^{31}P NMRS data were processed as previously described (11), using AMARES (34) in jMRUI (35) for the deconvolution of the two inorganic phosphate (P_i) resonances, and Topspin (Bruker Medical GMbG, Ettlingen, Germany) for the determination of PME (phosphomonoesters) and PDE (phosphodiesters). The following resonances were quantified: PME, $P_{i,b}$ (alkaline inorganic phosphate), $P_{i,a}$ (cytosolic inorganic phosphate), $P_{i,tot} = P_{i,b} + P_{i,a}$ (total inorganic phosphate), PDE, PCr (phosphocreatine), γATP, αATP, NAD(H) (nicotinamide adenine dinucleotide) and βATP (adenosine triphosphate) (11). Prior knowledge was imposed on signal amplitude, line width, phases and line shape (11). All metabolites were expressed as metabolite ratios, corrected for partial saturation. The (weighted) pH_w value was calculated based on the chemical shift difference between PCr and the P_i resonances (36). The intramuscular Mg^{2+} concentration was calculated based on the chemical shift difference between αATP and βATP (37,38). In *Figure 1*, two examples of ^{31}P NMR spectra are given for patients with a different disease progression.

Statistical analysis

Statistical analyses were conducted using SPSS software version 22 (SPSS, Chicago, IL, USA). Given the small number of patients, non-parametric tests were performed, including the Mann-Whitney test for comparing control and patient values and the Wilcoxon test for comparing sides and 1-year differences. Ambulant and non-ambulant patients were pooled for all analyses. The Spearman-rank correlation test was used for investigating the relationship between variables reflecting 'disease activity' (water T_2 and ^{31}P NMRS) and the earlier assessed indices of disease progression (19). Water T_2 values and ^{31}P NMRS indices used for correlation analyses are presented as the average value between the baseline and year-1 visit. The level of statistical significance was corrected for multiple comparisons and set at P<0.007 and at P<0.02, for NMRI and ^{31}P NMRS parameters, respectively.

The standardized response mean (SRM) is defined as the mean change over 1 year divided by the standard deviation of this change (39). An SRM ≥0.8 is considered to reflect a high responsiveness to change (39). For variables that are known to be less integrative but are, nevertheless, significantly different between the pathological and normal state, the standard SRM calculation is less pertinent. Therefore, we introduced an additional variable for the disease activity indices, which we further will call the 'standardized difference mean' (SDM). The SDM is defined
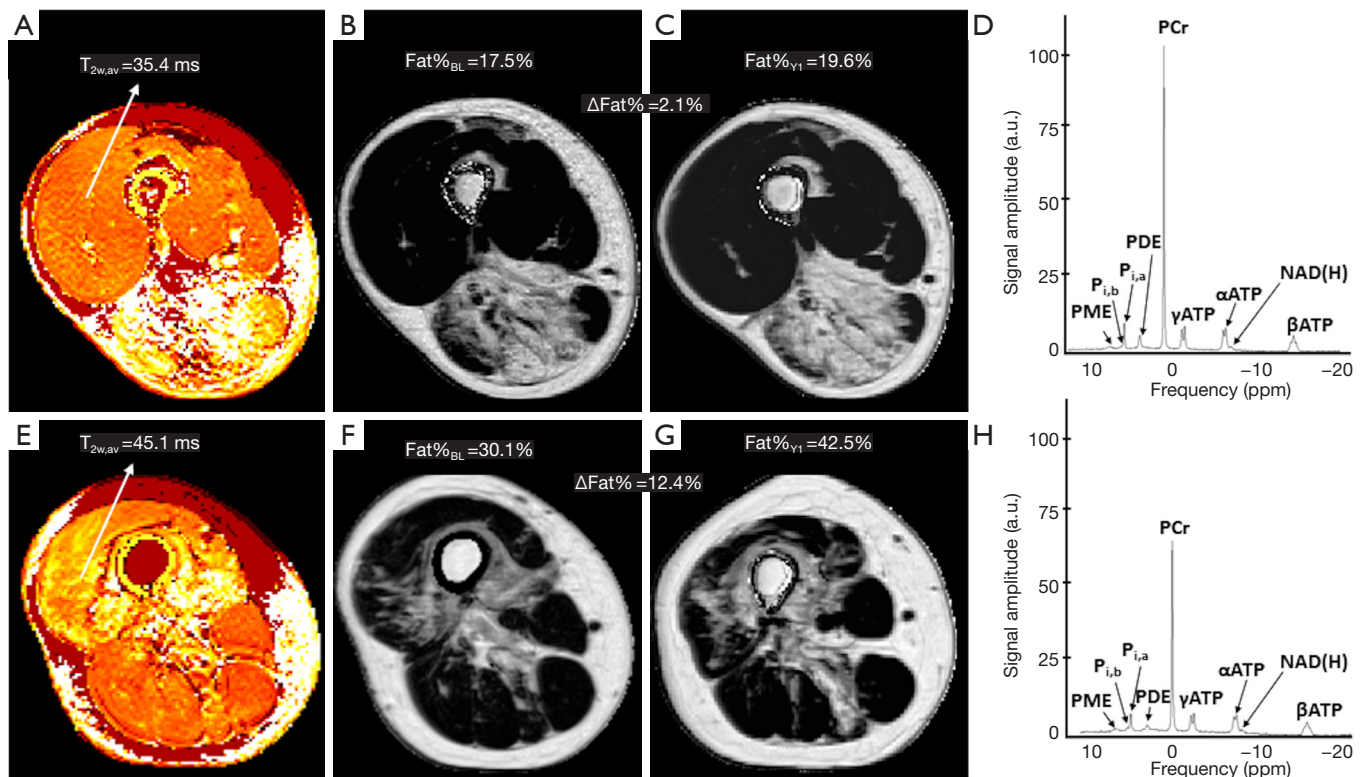
Figure 1 MSME-based baseline water T_2 maps (A,E), Dixon-based baseline (B,F), year-1 Fat% maps (C,G) and baseline QUAD ³¹P NMR spectra (D,H) of two GNE myopathy patients. Values for water T_2, Fat%$_{BL}$, Fat%$_{Y1}$ and ΔFat% in QUAD are given. In the first patient, water T_2 was normal (A), Fat%$_{BL}$ was relatively low (B), ΔFat% was the lowest of all patients (B,C), and PCr/γATP and pH$_w$ values were normal (D). In the second patient, water T_2 was abnormal (E), Fat%$_{BL}$ was intermediate (F), ΔFat% was the highest of all patients (F,G), and PCr/γATP and pH$_w$ values were significantly decreased and increased (H), respectively, as compared to controls. Notice that HSTR muscles shows much higher fatty depositions in the first and much less in the second patient. ATP, adenosine triphosphate; Fat%$_{BL}$, baseline fat fraction; Fat%$_{Y1}$, year-1 fat fraction; MSME, multi-slice multi-echo; NAD(H), nicotinamide adenine dicnucleotide; PCr, phosphocreatine; PDE, phosphodiesters; P$_{i,a}$, cytosolic inorganic phosphate; P$_{i,b}$, alkaline inorganic phosphate; PME, phosphomonoesters; T$_{2w,av}$, average water T_2 value; ΔFat%, fat fraction difference between baseline and year-1 visit.

as the sum of the mean change over 1 year and the mean difference between the patient and control group, divided by the pooled standard deviation of the 1-year change. Similar as for the SRM, an SDM ≥0.8 is considered to reflect a strong measurable difference from normality.

Results

Data overview

Quantitative NMRI data were obtained in the dominant forearm and the thigh of all ten GNEM patients. In four of the ten patients, no quantitative NMRI data were obtained in the leg due to overall Fat% values that were higher than 60%, as assessed by the whole-body Dixon measurement at

the beginning of the NMR protocol. Three of these four patients were non-ambulant.

³¹P NMRS measurements were performed at the level of the QUAD in all ten GNEM patients. In four of the ten patients (including the three non-ambulant subjects), ³¹P NMRS was not obtained in the HSTR, due to very high Fat% values in HSTR muscles. A fourth patient felt discomfort and the NMR protocol was ended before the ³¹P NMRS measurement in the HSTR.

'Disease progression' NMR indices in patients

As can be observed from *Table 1*, changes in Fat% were significant for the QUAD. No other significant changes

Table 1 Quantitative NMRI indices of disease progression ΔFat% and ΔcCSA (expressed as a mean and standard deviation)

Muscle group	ΔFat% (%)	ΔcCSA (cm^2)
Leg		
FIB	2.8±3.4	−0.3±0.3
EXT	4.9±3.5	−0.5±0.4
TRIC	1.5±3.7	−1.3±1.2
Thigh		
QUAD	3.1±2.1*	−2.4±2.8
HSTR	0.2±2.4	−1.0±1.1
Forearm		
EXT	0.5±3.0	−0.4±0.5
FLEX	0.5±2.7	−0.5±0.7

ΔFat%, Fat% change between baseline and year-1 (in %); ΔcCSA, absolute change in contractile cross-sectional area change between baseline and year-1 (in mm^2); EXT, extensor; FIB, fibularis; FLEX, flexor; HSTR, hamstring; QUAD, quadriceps; TRIC, triceps surae. Significance level: *, P<0.007.
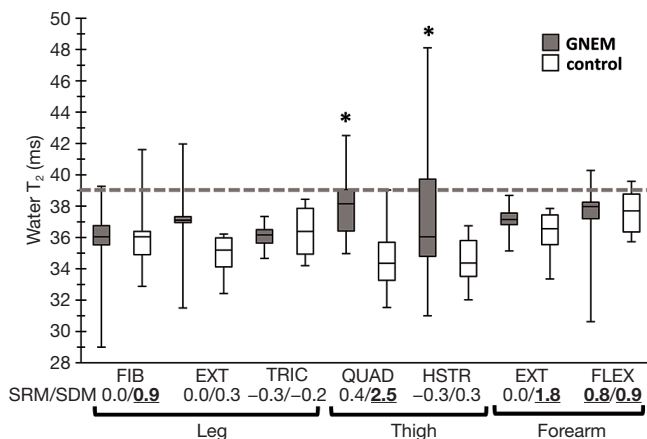

Figure 2 Box-and-whisker plots of water T_2 at baseline. The horizontal line represents an empirically determined threshold water T_2 value at 39 ms (i.e., the mean value plus twice the standard deviation of water T_2 in normal muscle) (31). SRM and SDM values ≥0.8 are indicated in bold. EXT, extensor; FIB, fibularis; FLEX, flexor; HSTR, hamstring; QUAD, quadriceps; SDM, standardized difference mean; SRM, standardized response mean; TRIC, triceps surae. Significance level: *P<0.007.

were observed.

Changes in 'disease activity' NMR indices between patients and controls

No significant age differences were found between patients and controls (P=0.292). There were no differences between left and right sides for water T_2 values (P>0.05 for all muscles).

Compared to controls, significantly higher water T_2 values (*Figure 2*) were only found in QUAD and HSTR muscles of GNEM patients, as depicted in *Figure 2*. SDM values for water T_2 were high for QUAD, FIB and forearm muscles. No significant differences between muscles were observed for the average water T_2 values in both patients and controls (P>0.05).

Additionally, anomalies in various ^{31}P NMRS indices were observed in QUAD and HSTR as compared to controls (*Figure 3*). Corresponding SDM values for all depicted ^{31}P NMRS indices were all higher than 0.8.

Significant differences between QUAD and HSTR were only found for pH in the healthy controls (7.08±0.03 *vs.* 7.05±0.02, P=0.003) and for PCr/γATP (5.56±0.39 *vs.* 4.89±0.33, P=0.016) in GNEM patients.

Changes in 'disease activity' NMR indices in patients after 1 year

Water T_2 did not change after one year of follow-up. The SRM value in FLEX_FOREARM reached 0.8 but water T_2 changes were non-significant (37.3±2.6 to 39.5±2.0 ms, P=0.022).

A few ^{31}P NMRS indices changed significantly over the course of one year, such as increases in pH$_w$ (7.08±0.03 *vs.* 7.10±0.03, P=0.012, SRM =1.6) and PME/γATP (0.27±0.04 *vs.* 0.33±0.07, P=0.014, SRM =1.0) in QUAD. SRM reached 0.8 in HSTR for PME/γATP but changes were, however, non-significant after 1 year.

Correlations between 'disease activity' and 'disease progression' NMR indices

All correlation coefficients and corresponding P-values can be found in *Table 2*.

In QUAD, ΔFat% correlated significantly with water T_2 (*Figure 4*). This significance was even more pronounced when correlating water T_2 with the R_{muscle_transf} index, as seen in *Figure 4B*. Water T_2 values in QUAD seemed to be correlated (albeit non-significant) with the relative ΔcCSA
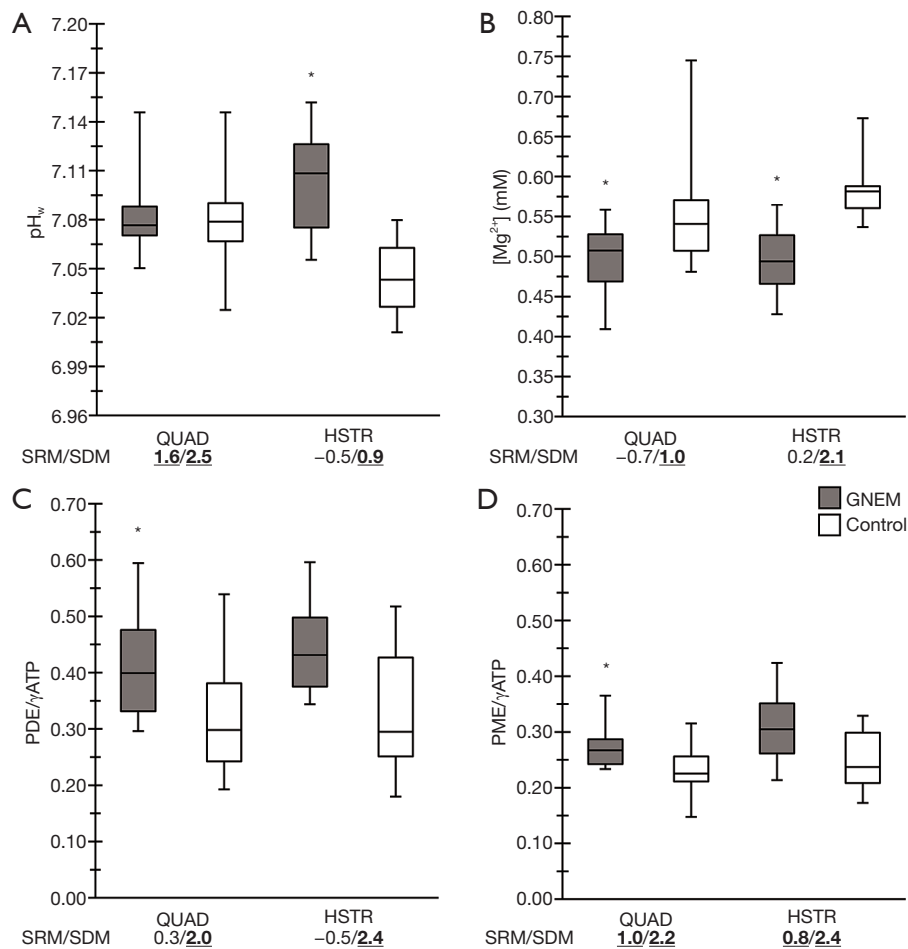
Figure 3 Box-and-whisker plots of pH$_w$ (A), [Mg^{2+}] (B), PDE/γATP (C) and PME/γATP (D) at baseline in QUAD and HSTR. SRM and SDM values ≥0.8 are indicated in bold. ATP, adenosine triphosphate; HSTR, hamstring; [Mg^{2+}], intramuscular magnesium concentration (in mM); pH$_w$, weighted pH; PDE, phosphomonoesters; PME, phosphomonoesters; QUAD, quadriceps; SDM, standardized difference mean; SRM, standardized response mean; significance level: *P<0.02.

values, as illustrated in *Figure 4D*. Additionally, significant correlations were found between PCr/γATP and ΔcCSA and ΔcCSA$_{rel}$ in QUAD (*Figure 5*).

Discussion

This study demonstrates that water T$_2$ and ^{31}P NMRS have a predictive value on the progression of disease in skeletal muscles as established by fat-water separation-based quantitative NMRI in GNEM patients.

'Disease progression': ΔFat% and ΔcCSA

The extent of muscle destruction in GNEM, as reflected

by the increased fatty infiltration and decreased lean muscle tissue as compared to controls, was especially evident in the thigh (QUAD and HSTR) and the extensor compartment of the leg, with a relative sparing of the QUAD muscle group as compared to the other muscles (19), confirming observations from earlier reports (3). Disease progression in GNEM, illustrated by both an increase in fatty depositions (ΔFat%) and a decrease in lean muscle tissue (ΔcCSA), was also seen in these three muscle groups (although only significant changes were seen for Fat% in QUAD). In general, all leg muscles in GNEM patients were heavily fatty infiltrated, confirming the distal-to-proximal disease evolution known in GNEM (40). Disease progression indices were handled in detail in a separate publication (19).
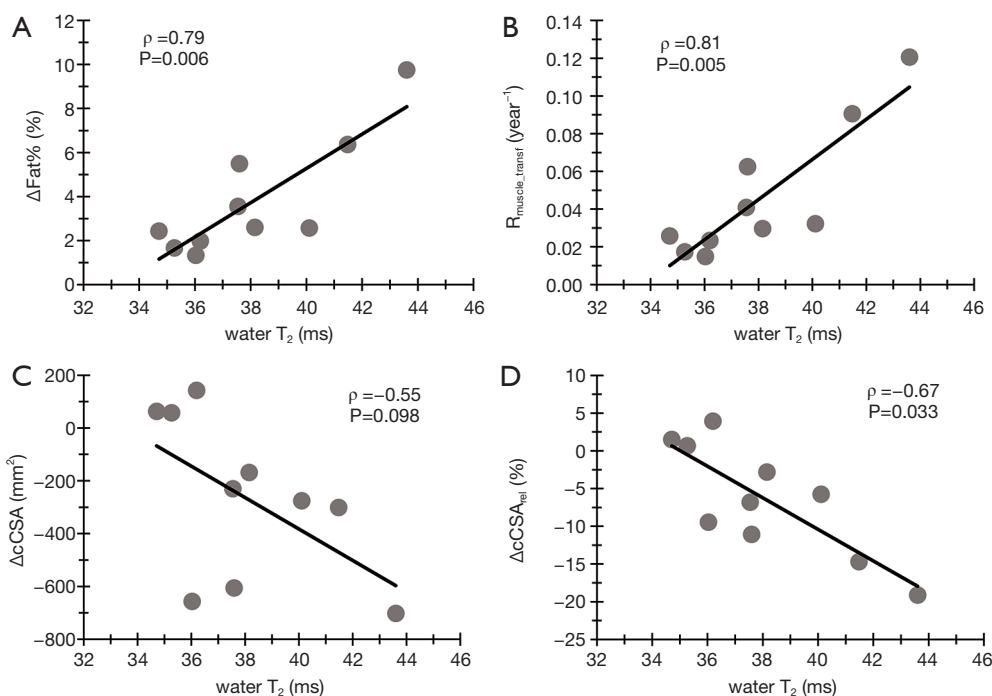
Figure 4 All 'disease progression' NMRI indices as a function of water T_2 in QUAD. Every point represents 1 patient. The water T_2 value represents the average value of baseline and year 1 visits (the analysis with baseline water T_2 values resulted in the same outcome for ρ and P values). See *Table 2* for Spearman correlation coefficients (ρ) and corresponding P values. ΔFat%, fat fraction change between baseline and year-1 (in %); ΔcCSA, absolute change in contractile cross-sectional area change between baseline and year-1 (in mm^2); ΔcCSA$_{rel}$, relative change in contractile cross-sectional area change between baseline and year-1 (in %); R$_{muscle\_transf}$, muscle transformation rate (year^{-1}). Significance level: *P<0.007.

'Disease activity': water T_2

An increase in water T_2 might be related to different phenomena such as inflammation, myocytic lesions, cell necrosis or edema, and can therefore be regarded as a non-specific NMR biomarker reflecting 'disease activity' (10). Whereas the abovementioned variables, Fat% and cCSA, are more integrators of the global disease progression over time, water T_2 reflects a more instantaneous phenomenon.

The significantly increased water T_2, as found in this study in 25% of all QUAD and HSTR muscles, might be perceived as surprising, as it is known that inflammation is generally absent in GNEM (3). A similar apparent paradox has been observed in late-onset Pompe disease patients (17) where the increased water T_2 could not be associated to an inflammatory cause, from which it is hypothesized that the abnormal water T_2 values rather reflect myocytic lesions, possibly related to the rupture of lysosomes. In the patients assessed in our study, a significantly increased water T_2 was only found in the thigh. This could be due to a lack of

statistical power since leg data were not acquired in four of the ten patients due to very high Fat% levels (19). EXT_FOREARM muscles revealed to have an SDM similar as found in thigh, illustrating its potential as a muscle where water T_2 might be significantly different between healthy and pathological muscle tissue. GNEM patients did not show any significant change in water T_2 over a 1-year time period, which does not rule out fluctuations between these two time points. Altogether, these data indicate that the well-preserved QUAD is the most appropriate muscle group to assess disease evolution through water T_2 measurements in GNEM.

'Disease activity': ^{31}P NMRS

Although inter-patient differences in ^{31}P NMRS indices were apparent, significant differences as compared to controls were found for only a few of these parameters. One of the prominent differences were the elevated levels of PDE, found in QUAD and HSTR, which reflects an

Table 2 Correlations between predictive 'disease activity' and 'disease progression' NMR indices (the Spearman-rank correlation coefficient ρ is given with the P value between brackets; n indicates the number of patients)

Muscle group	n	ΔFat% (%)	R$_{muscle\_transf}$ (year^{-1})	ΔcCSA (mm^2)	ΔcCSA$_{rel}$ (%)
Water T$_2$ (ms)					
FIB (leg)	6	−0.37 (0.468)	−0.26 (0.623)	0.77 (0.072)	0.26 (0.623)
EXT (leg)	6	0.54 (0.266)	0.20 (0704)	−0.89 (0.019)	−0.66 (0.156)
TRIC (leg)	6	−0.37 (0.468)	−0.31 (0.544)	0.09 (0.872)	0.37 (0.468)
QUAD (thigh)	10	0.79 (0.006)	0.81 (0.005)	−0.55 (0.098)	−0.67 (0.033)
HSTR (thigh)	10	−0.27 (0.446)	−0.19 (0.603)	0.58 (0.200)	−0.03 (0.934)
EXT (forearm)	10	0.51 (0.130)	0.53 (0.119)	−0.31 (0.379)	−0.44 (0.199)
FLEX (forearm)	10	0.10 (0.783)	0.10 (0.783)	−0.54 (0.109)	−0.38 (0.285)
pH$_w$					
QUAD	10	0.09 (0.803)	0.10 (0.777)	−0.03 (0.934)	0.01 (0.987)
HSTR	6	−0.03 (0.957)	0.20 (0.704)	0.09 (0.872)	−0.66 (0.156)
[Mg^{2+}] (mM)					
QUAD	10	−0.18 (0.627)	−0.22 (0.533)	0.71 (0.022)	0.53 (0.117)
HSTR	6	−0.03 (0.957)	−0.31 (0.544)	−0.49 (0.329)	0.37 (0.468)
PDE/γATP					
QUAD	10	−0.19 (0.603)	−0.25 (0.489)	0.18 (0.627)	0.30 (0.405)
HSTR	6	−0.37 (0.468)	−0.49 (0.329)	0.54 (0.266)	0.60 (0.208)
PME/γATP					
QUAD	10	0.59 (0.074)	0.60 (0.067)	−0.10 (0.777)	−0.24 (0.511)
HSTR	6	0.31 (0.544)	0.54 (0.266)	0.09 (0.872)	−0.77 (0.072)
PCr/γATP					
QUAD	10	−0.58 (0.082)	−0.53 (0.117)	0.73 (0.016)	0.78 (0.008)
HSTR	6	−0.83 (0.042)	−0.88 (0.019)	0.09 (0.872)	0.60 (0.208)
P$_{i,tot}$/γATP					
QUAD	10	−0.02 (0.960)	0.07 (0.855)	−0.19 (0.603)	−0.16 (0.651)
HSTR	6	−0.49 (0.329)	−0.20 (0.704)	0.09 (0.872)	−0.09 (0.872)
P$_{i,tot}$/PCr					
QUAD	10	0.43 (0.214)	0.50 (0.138)	−0.65 (0.043)	−0.61 (0.060)
HSTR	6	−0.43 (0.397)	−0.09 (0.872)	−0.26 (0.623)	−0.49 (0.329)
P$_{i,b}$/P$_{i,tot}$					
QUAD	10	0.22 (0.533)	0.21 (0.556)	−0.14 (0.701)	−0.25 (0.489)
HSTR	6	−0.26 (0.623)	−0.43 (0.397)	−0.09 (0.872)	−0.03 (0.957)

The water T$_2$ value and the ^{31}P NMR indices represent the average value of baseline and year 1 visits (the analysis with baseline water T$_2$ values resulted in the same outcome for ρ and P values). ΔFat%, Fat% change between baseline and year-1 (in %); ΔcCSA, absolute change in contractile cross-sectional area change between baseline and year-1 (in mm^2); ΔcCSA$_{rel}$, relative change in contractile cross-sectional area change between baseline and year-1 (in %); ATP, adenosine triphosphate; EXT, extensor; FIB, fibularis; FLEX, flexor; HSTR, hamstring; PDE, phosphodiesters; PCr, phosphocreatine; P$_{i,b}$, alkaline inorganic phosphate; P$_{i,tot}$, total inorganic phosphate; PME, phosphomonoesters; QUAD, quadriceps; [Mg^{2+}], intramuscular magnesium concentration (in mM); pH$_w$, weighted pH; R$_{muscle\_transf}$, muscle transformation rate (year^{-1}). Significance levels: P<0.007 (NMRI) and P<0.02 (^{31}P NMRS).
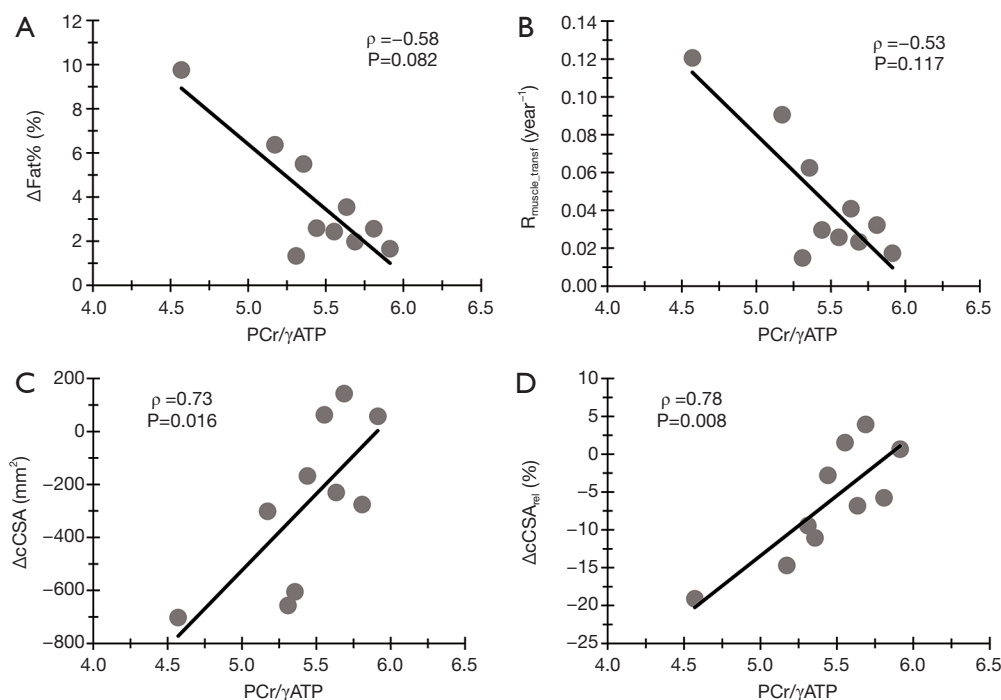
Figure 5 ΔFat% (A), R_{muscle_transf} (B) ΔcCSA (C) and ΔcCSA$_{rel}$ (D) as a function of PCr/γATP in QUAD. Every point represents 1 patient. All ^{31}P NMR indices represent the average value of baseline and year 1 visits (the analysis with baseline water T_2 values resulted in the same outcome for ρ and P values). See *Table 2* for Spearman correlation coefficients (ρ) and corresponding P values. ΔFat%, fat fraction change between baseline and year-1 (in %); ΔcCSA, absolute change in contractile cross-sectional area change between baseline and year-1 (in mm^2); ΔcCSA$_{rel}$, relative change in contractile cross-sectional area change between baseline and year-1 (in %); ATP, adenosine triphosphate; PCr, phosphocreatine; R_{muscle_transf}, muscle transformation rate (year^{-1}). Significance level: *P<0.02.

increased turnover of phospholipids, indicating a metabolic disturbance at the level of the sarcolemmal membrane (41). Both in BMD and DMD, PDE was found to be an early marker during the disease, as changes were observed prior to any other NMR-detectable changes such as Fat% (12,14). When comparing our results to those of the BMD study where the patient age range (i.e., 20–60 years) was similar to the one in this work (i.e., 25–73 years), we can, however, not assess the possibility of PDE as an early-phase biomarker of the disease, since the relatively spared QUAD demonstrated already low to moderate fat replacement (i.e., between 4.3% and 29.7%) (19). Additionally, it is known that PDE correlates positively with age (42,43), making age a confounding factor for further interpretation. Also, an elevated pH value was found in the HSTR and QUAD (at least at year 1), when comparing to the controls. An alkaline pH has shown to be a biomarker for dystrophic muscle, as illustrated in several studies already, with a normal pH in non-fat infiltrated DMD patients (12) compared to an alkaline pH when muscle began to show fatty replacement

(11,12,20). An elevated pH reflects an increase in the second more alkaline P_i pool ($P_{i,b}$), which is hypothesized to originate from suffering myocytes or from an expanded interstitial space, as was demonstrated in dystrophic muscle (11,20). Increased PDE, as a marker of membrane disturbance, could result from abnormal or insufficient glycosylation/sialylation of important transmembrane glycoproteins, such as the voltage-gated sodium channels or α-dystroglycan as part of the dystrophin-glycoprotein complex (44). Dysfunction of these proteins could result in a reduced mechanostability of the sarcolemma, causing leaky membranes and a disturbed ionic homeostasis with implications on the value of pH. Further studies are required to investigate the dynamics of pH and PDE before the occurrence of fatty depositions in the muscle of GNEM patients. Finally, a significantly decreased intramuscular Mg^{2+} content, as was observed in both QUAD and HSTR, is also an interesting finding, knowing that Mg^{2+} is an essential and one of the most effective metal ions with respect to the activity of N-acetylmannosamine kinase activity, being

one of the two GNE-coded enzymes (45,46). Despite the difference in Fat% between QUAD and HSTR (4.3–29.7% and 8.1–86.4%, respectively) (19), only the PCr/γATP ratio was shown to differ significantly between the two muscle groups. This illustrates that the very different extent of fatty infiltration in these muscle groups (at least up until a certain threshold) seemed to have, on average, little effect on the outcome of these parameters, whereas this correlation has been observed earlier in FSHD (47) and DMD (11). Significant changes coupled to high SRM values were only found for pH, PME/γATP and PCr/γATP in QUAD. This doesn't rule out, nevertheless, the use of Mg^{2+} and PDE/γATP as biomarkers that are potentially subjective to treatment effects, since they show, just as pH and PME/γATP, a high degree of discriminative power between patients and controls (SDM ≥0.8) in both QUAD and HSTR.

Relationship between 'disease activity' and 'disease progression'

We demonstrated that QUAD muscles of GNEM patients with abnormal water T$_2$ experienced a faster disease progression, as seen with most variables reflecting 'disease progression'. A similar relationship was observed in late-onset Pompe disease patients (17) where an elevated water T$_2$ implied a doubling of the fatty infiltration rate. Along the same line, convincing evidence have been repeatedly produced in FSHD, a disease where bursts of toxic gene expression and inflammation in a particular muscle result in its rapid destruction. Several studies have shown that muscle hyperintensities in STIR imaging or muscle water T$_2$ increases in quantitative maps precede muscle fatty replacement in T$_1$-weighted images or in fat fraction maps (48-50). Correlations between water T$_2$ and disease progression indices were less clear in other lower limb and forearm flexor muscles in this study, most plausibly due to the higher degree of fatty replacement in these muscles (19), making a reliable estimation of water T$_2$ more challenging (33). Also, fluctuations of water T$_2$ during the course of the study might have impacted the correlation. Therefore, the average value of both visits was used for the correlation analysis since it reflects better the oscillating nature of the muscle water T$_2$ during which the study was running. The PCr/γATP ratio, as a marker of metabolic efficiency of the (residual) muscle, was correlated with disease progression indices in the thigh muscles. In QUAD, a strong relationship between the macroscopic

loss of muscle mass as reflected by a reduction in cCSA, and biochemical changes such as the decreased PCr/γATP ratio reflecting a loss of contractile tissue, was shown in that specific muscle that is relatively spared but where disease activity is, nevertheless, high. In DMD, a positive correlation was established between PCr/γATP and the grip strength in FLEX_FOREARM (51), which, in its turn, is strongly correlated with the amount of muscle tissue, as illustrated in GNEM (19). In HSTR, where fatty infiltration was, on average, much more pronounced, similar correlations were observed, more indirectly, between PCr/γATP and R$_{muscle\_transf}$, but not with cCSA changes. Finally, the tendency of correlation found between intramuscular Mg^{2+} and the loss in QUAD tissue suggests that Mg^{2+} could be a potential biomarker in future therapeutic interventions in GNEM.

A recent phase-3 trial demonstrated that the extended-release formulation of sialic acid did not improve muscle strength and function in GNEM patients, as compared to placebo-treated GNEM patients (52), although it should be mentioned that quantitative NMRI and ^{31}P NMRS variables were not assessed in these patients. The study outcome might have been different, however, if these variables had been measured. While quantitative NMRI and several functional quantitative biomarkers have illustrated to be highly sensitive to disease progression, the regulatory agencies are still requesting evidence of a tangible clinical effect for a new treatment to be validated. There are many observations supporting the following chain of events in muscle disease: (I) muscle damage, (II) muscle destruction and fatty replacement, (III) strength loss, (IV) functional impairment, and finally (V) disability. The formal demonstration of this cascade is extremely challenging, though, because of the time-scale in most diseases. A normalization of water T$_2$ or halting the muscle fatty replacement as measured with quantitative NMRI, reflecting an interruption of the succession of pathological mechanisms leading to disability, are both potential strong indicators of a successful therapeutic intervention.

Methodological aspects

The major methodological issue in this study was the combination of the limited amount of patients, which is due to the very low prevalence of the disease (estimated 1/1,000,000 worldwide) (3) and the heterogeneous phenotype inherent to the disease, emphasizing even more the need for objective outcome measures. Because the

ambulant and non-ambulant cohorts were too small for a paired ambulant versus non-ambulant analysis, data were pooled. Despite the low number of patient data, however, we were able to detect significant changes and correlations in skeletal muscle over a 1-year period using quantitative NMRI and ^{31}P NMRS. Nevertheless, more data is needed to confirm and verify correlations between 'disease prediction' and 'disease progression' NMR indices, since above a certain threshold of fatty infiltration (approximately 50%), water T_2 assessment becomes unreliable (33) and ^{31}P NMRS does not reach a sufficient signal-to-noise level due to lack of viable muscle tissue, as was, for example, the case for HSTR in this study.

Conclusions

To summarize, this study revealed that, in GNEM, water T_2 and ^{31}P NMRS are complementary NMR indices to the standard Fat% assessment for evaluating muscle changes during the course of the disease. More specifically, the QUAD, which is relatively preserved in GNEM, in patients with higher water T2 values showed a faster disease progression. The results obtained in this study confirm the ability of the use of water T_2 and ^{31}P NMRS as possible surrogate endpoints in longitudinal studies of neuromuscular disorders. Future steps could be the implementation of this quantitative NMR protocol in a larger patient cohort as well as in clinical trials before and after a suitable treatment.

Acknowledgments

Footnote

Conflicts of Interest: All authors have completed the ICMJE uniform disclosure form (available at http://dx.doi.org/10.21037/qims-20-39). AB reports personal fees from Ultragenyx pharmaceutical, during the conduct of the study;

LS reports grants and personal fees from Avexis, grants and personal fees from Biogen, grants and personal fees from Roche, personal fees from Cytokinetics, personal fees from Sarepta, personal fees from Biophytis, personal fees from Pfizer, personal fees from Catabasis, personal fees from Lupin, grants and personal fees from Dynacure, personal fees from Audentes, outside the submitted work; PGC reports personal fees from Santhera, personal fees from Sanofi, personal fees from Sarepta, outside the submitted work. The authors have no other conflicts of interest to declare.

Ethical Statement: Healthy control subjects were scanned as part of a methodology NMRI/S protocol approved by the local ethics committee (CPP-Ile de France VI – Groupe Hospitalier Pitié-Salpêtrière, ID RCB: 2012-A01689-34) and informed consent was obtained from all controls and patients.

References

1. Eisenberg I, Avidan N, Potikha T, Hochner H, Chen M, Olender T, Barash M, Shemesh M, Sadeh M, Grabov-Nardini G, Shmilevich I, Friedmann A, Karpati G, Bradley WG, Baumbach L, Lancet D, Asher E Ben, Beckmann JS, Argov Z, Mitrani-Rosenbaum S. The UDP-N-acetylglucosamine 2-epimerase/N-acetylmannosamine kinase gene is mutated in recessive hereditary inclusion body myopathy. Nat Genet 2001;29:83-7.
2. Schauer R. Sialic acids: Fascinating sugars in higher animals and man. Zoology 2004;107:49-64.
3. Nishino I, Carrillo-Carrasco N, Argov Z. GNE myopathy: current update and future therapy. J Neurol Neurosurg Psychiatry 2015;86:385-92.
4. Malicdan MC V, Noguchi S, Nonaka I, Hayashi YK, Nishino I. A Gne knockout mouse expressing human GNE D176V mutation develops features similar to distal myopathy with rimmed vacuoles or hereditary inclusion

1462

Reyngoudt et al. Water T$_2$ NMRI and ^{31}P NMRS in skeletal muscle in GNE myopathy

body myopathy. Hum Mol Genet 2007;16:2669-82.

5. Nonaka I, Noguchi S, Nishino I. Distal myopathy with rimmed vacuoles and hereditary inclusion body myopathy. Curr Neurol Neurosci Rep 2005;5:61-5.

6. Tasca G, Ricci E, Monforte M, Laschena F, Ottaviani P, Rodolico C, Barca E, Silvestri G, Iannaccone E, Mirabella M, Broccolini A. Muscle imaging findings in GNE myopathy. J Neurol 2012;259:1358-65.

7. Chu CC, Kuo HC, Yeh TH, Ro LS, Chen SR, Huang CC. Heterozygous mutations affecting the epimerase domain of the GNE gene causing distal myopathy with rimmed vacuoles in a Taiwanese family. Clin Neurol Neurosurg 2007;109:250-6.

8. Chaouch A, Brennan KM, Hudson J, Longman C, McConville J, Morrison PJ, Farrugia ME, Petty R, Stewart W, Norwood F, Horvath R, Chinnery PF, Costigan D, Winer J, Polvikoski T, Healy E, Sarkozy A, Evangelista T, Pogoryelova O, Eagle M, Bushby K, Straub V, Lochmüller H. Two recurrent mutations are associated with GNE myopathy in the North of Britain. J Neurol Neurosurg Psychiatry 2014;85:1359-65.

9. de Dios JKL, Shrader JA, Joe GO, McClean JC, Williams K, Evers R, Malicdan MCV, Ciccone C, Mankodi A, Huizing M, McKew JC, Bluemke DA, Gahl WA, Carrillo-Carrasco N. Atypical presentation of GNE myopathy with asymmetric hand weakness. Neuromuscul Disord 2014;24:1063-7.

10. Carlier PG, Marty B, Scheidegger O, Loureiro de Sousa P, Baudin P-Y, Snezhko E, Vlodavets D. Skeletal muscle quantitative nuclear magnetic resonance imaging and spectroscopy as an outcome measure for clinical trials. J Neuromuscul Dis 2016;3:1-28.

11. Wary C, Azzabou N, Giraudeau C, Le Louër J, Montus M, Voit T, Servais L, Carlier P. Quantitative NMRI and NMRS identify augmented disease progression after loss of ambulation in forearms of boys with Duchenne muscular dystrophy. NMR Biomed 2015;28:1150-62.

12. Hooijmans MT, Niks EH, Burakiewicz J, Verschuuren JJGM, Webb AG, Kan HE. Elevated phosphodiester and T2 levels can be measured in the absence of fat infiltration in Duchenne muscular dystrophy patients. NMR Biomed 2017;30:e3667.

13. Willcocks RJ, Rooney WD, Triplett WT, Forbes SC, Lott DJ, Senesac CR, Daniels MJ, Wang DJ, Harrington AT, Tennekoon GI, Russman BS, Finanger EL, Byrne BJ, Finkel RS, Walter GA, Sweeney HL, Vandenborne K. Multicenter prospective longitudinal study of magnetic resonance biomarkers in a large Duchenne muscular

dystrophy cohort. Ann Neurol 2016;79:535-47.

14. Wokke BH, Hooijmans MT, van den Bergen JC, Webb AG, Verschuuren JJ, Kan HE. Muscle MRS detects elevated PDE/ATP ratios prior to fatty infiltration in Becker muscular dystrophy. NMR Biomed 2014;27:1371-7.

15. Kan HE, Scheenen TWJ, Wohlgemuth M, Klomp DWJ, van Loosbroek-Wagenmans I, Padberg GW, Heerschap A. Quantitative MR imaging of individual muscle involvement in facioscapulohumeral muscular dystrophy. Neuromuscul Disord 2009;19:357-62.

16. Willis TA, Hollingsworth KG, Coombs A, Sveen ML, Andersen S, Stojkovic T, Eagle M, Mayhew A, de Sousa PL, Dewar L, Morrow JM, Sinclair CD, Thornton JS, Bushby K, Lochmüller H, Hanna MG, Hogrel JY, Carlier PG, Vissing J, Straub V. Quantitative muscle MRI as an assessment tool for monitoring disease progression in LGMD2I: a multicentre longitudinal study. PLoS One 2013;8:e70993.

17. Carlier PG, Azzabou N, de Sousa PL, Hicks A, Boisserie JM, Amadon A, Carlier RY, Wary C, Orlikowski D, Laforêt P. Skeletal muscle quantitative nuclear magnetic resonance imaging follow-up of adult Pompe patients. J Inherit Metab Dis 2015;38:565-72.

18. Morrow JM, Sinclair CDJ, Fischmann A, Machado PM, Reilly MM, Yousry TA, Thornton JS, Hanna MG. MRI biomarker assessment of neuromuscular disease progression: a prospective observational cohort study. Lancet Neurol 2016;15:65-77.

19. Gidaro T, Reyngoudt H, Le Louër J, Behin A, Toumi F, Villeret M, Araujo ECA, Baudin PY, Marty B, Annoussamy M, Hogrel JY, Carlier PG, Servais L. Quantitative nuclear magnetic resonance imaging detects subclinical changes over 1 year in skeletal muscle of GNE myopathy. J Neurol 2020;267:228-38.

20. Reyngoudt H, Turk S, Carlier PG 1H NMRS of carnosine combined with 31P NMRS to better characterize skeletal muscle pH dysregulation in Duchenne muscular dystrophy. NMR Biomed 2018;31:e3839.

21. Park JH, Vansant JP, Kumar NG, Gibbs SJ, Curvin MS, Price RR, Partain CL, James AE. Dermatomyositis: Correlative MR imaging and P-31 MR spectroscopy for quantitative characterization of inflammatory disease. Radiology 1990;177:473-9.

22. Maillard SM, Jones Jones R, Owens C, Pilkington C, Woo P, Wedderburn LR, Murray KJ. Quantitative assessment of MRI T2 relaxation time of thigh muscles in juvenile dermatomyositis. Rheumatology (Oxford) 2004;43:603-8.

23. Walker UA. Imaging tools for the clinical assessment

of idiopathic inflammatory myositis. Curr Opin Rheumatol.2008;20:656-61.

24. Degardin A, Morillon D, Lacour A, Cotten A, Vermersch P, Stojkovic T. Morphologic imaging in muscular dystrophies and inflammatory myopathies. Skeletal Radiol 2010;39:1219-27.

25. Yao L, Gai N. Fat-corrected T2 measurements as a marker of muscle disease in inflammatory myopathy. Am J of Roentgenol 2012;198:475-81.

26. Carlier PG, Azzabou N, de Sousa PL, Florkin B, Deprez E, Romero NB, Denis S, Decostre V, Servais L. Diagnostic role of quantitative NMR imaging exemplified by 3 cases of juvenile dermatomyositis. Neuromuscul Disord 2013;23:814.

27. Mankodi A, Azzabou N, Bulea T, Reyngoudt H, Shimellis H, Ren Y, Kim E, Fischbeck KH, Carlier PG. Skeletal muscle water T2 as a biomarker of disease status and exercise effects in patients with Duchenne muscular dystrophy. Neuromuscul Disord 2017;27:705-14.

28. Marty B, Baudin PY, Reyngoudt H, Azzabou N, Araujo ECA, Carlier PG, de Sousa PL. Simultaneous muscle water T2 and fat fraction mapping using transverse relaxometry with stimulated echo compensation. NMR Biomed 2016;29:431-43.

29. Bachasson D, Reyngoudt H, Turk S, Benveniste O, Hogrel JY, Carlier PG. Muscle alterations in sporadic inclusion body myositis assessed using quantitative nuclear magnetic resonance imaging and spectroscopy, ultrasound shear-wave elastography, and relationships with muscle function. Neuromuscul Disord 2017;27:S123.

30. Azzabou N, Hogrel JY, Carlier PG. NMR based biomarkers to study age-related changes in the human quadriceps. Exp Gerontol 2015;70:54-60.

31. Baudin PY, Marty B, Robert B, Shukelovitch A, Carlier RY, Azzabou N, Carlier PG. Qualitative and quantitative evaluation of skeletal muscle fatty degenerative changes using whole-body Dixon nuclear magnetic resonance imaging for an important reduction of the acquisition time. Neuromuscul Disord 2015;25:758-63.

32. Amadon A, Cloos MA, Boulant N, Hang MF, Wiggins CJ, Fautz HP. Validation of a very fast B1-mapping sequence for parallel transmission on a human brain at 7T. Proc Intl Soc Mag Reson Med 2012;20:3358.

33. Azzabou N, de Sousa PL, Araujo EC, Carlier PG. Validation of a generic approach to muscle water T2 determination at 3T in fat-infiltrated skeletal muscle. J Magn Reson Imaging 2015;41:645-53.

34. Vanhamme L, van den Boogaart A, Van Huffel S.

Improved method for accurate and efficient quantification of MRS data with use of prior knowledge. J Magn Reson 1997;129:35-43.

35. Naressi A, Couturier C, Devos JM, Janssen M, Mangeat C, de Beer R, Graveron-Demilly D. Java-based graphical user interface for the MRUI quantitation package. MAGMA 2001;12:141-52.

36. Moon RB, Richards JH. Determination of intracellular pH by 31P magnetic resonance. J Biol Chem 1973;248:7276-8.

37. Wary C, Brillault-Salvat C, Bloch G, Leroy-Willig A, Roumenov D, Grognet JM, Leclerc JH, Carlier PG. Effect of chronic magnesium supplementation on magnesium distribution in healthy volunteers evaluated by 31P-NMRS and ion selective electrodes. Br J Clin Pharmacol 1999;48:655-62.

38. Reyngoudt H, Lopez Kolkovsky AL, Carlier PG. Free intramuscular Mg2+ concentration calculated using both 31P and 1H NMRS-based pH in skeletal muscle of Duchenne muscular dystrophy patients. NMR Biomed 2019;32:e4115.

39. Cohen J. Statistical power analysis for the behavioral sciences. Hillsdale: L. Erlbaum Associates, 1988.

40. Broccolini A, Gidaro T, Morosetti R, Mirabella M. Hereditary inclusion-body myopathy: Clues on pathogenesis and possible therapy. Muscle Nerve 2009;40:340-9.

41. Srivastava NK, Yadav R, Mukherjee S, Pal L, Sinha N. Abnormal lipid metabolism in skeletal muscle tissue of patients with muscular dystrophy: In vitro, high-resolution NMR spectroscopy based observation in early phase of the disease. Magn Reson Imaging 2017;38:163-73.

42. Younkin DP, Berman P, Sladky J, Chee C, Bank W, Chance B. 31P NMR studies in Duchenne muscular dystrophy: age-related metabolic changes. Neurology 1987;37:165-9.

43. Reyngoudt H, Marty B, Baudin PY, Azzabou N, Carlier PG. Multinuclear NMR spectroscopic biomarkers for energy metabolism characterization in aging skeletal muscle. J Cachexia Sarcopenia Muscle 2015;6:487.

44. Marini M, Ambrosini S, Sarchielli E, Thyrion GDZ, Bonaccini L, Vannelli GB, Sgambati E. Expression of sialic acids in human adult skeletal muscle tissue. Acta Histochem 2014;116:926-35.

45. Hinderlich S, Sonnenschein A, Reutter W. Metal ion requirement of bifunctional UDP-N-acetylglucosamine 2-epimerase/N-acetylmannosamine kinase from rat liver. BioMetals 1998;11:253-8.

46. Darvish D. Magnesium may help patients with recessive hereditary inclusion body myopathy, a pathological review.

Med Hypotheses 2003;60:94-101.

47. Kan HE, Klomp DWJ, Wohlgemuth M, van Loosbroek-Wagemans I, van Engelen BGM, Padberg GW, Heerschap A. Only fat infiltrated muscles in resting lower leg of FSHD patients show disturbed energy metabolism. NMR Biomed 2010;23:563-8.

48. Friedman SD, Poliachik SL, Otto RK, Carter GT, Budech CB, Bird TD, Miller DG, Shaw DW. Longitudinal features of STIR bright signal in FSHD. Muscle Nerve 2014;49:257-60.

49. Fatehi F, Salort-Campana E, Le Troter A, Lareau-Trudel E, Bydder M, Fouré A, Guye M, Bendahan D, Attarian S. Long-term follow-up of MRI changes in thigh muscles of patients with facioscapulohumeral dystrophy: A quantitative study. PLoS One 2017;12: e0183825.

50. Monforte M, Laschena F, Ottaviani P, Bagnato MR, Pichiecchio A, Tasca G, Ricci E. Tracking muscle wasting and disease activity in facioscapulohumeral musculardystrophy by qualitative longitudinal imaging. J Cachexia Sarcopenia Muscle 2019;10:1258-65.

51. Hogrel JY, Wary C, Moraux A, Azzabou N, Decostre V, Ollivier G, Canal A, Lilien C, Ledoux I, Annoussamy M, Reguiba N, Gidaro T, Le Moing AG, Cardas R, Voit T, Carlier PG, Servais L. Longitudinal functional and NMR assessment of upper limbs in Duchenne muscular dystrophy. Neurology 2016;86:1022-30.

52. Lochmüller H, Behin A, Caraco Y, Lau H, Mirabella M, Tournev I, Tarnopolsky M, Pogoryelova O, Woods C, Lai A, Shah J, Koutsoukous T, Skrinar A, Mansbach H, Kakkis E, Mozaffar T. A phase 3 randomized study evaluating sialic acid extended-release for GNE myopathy. Neurology 2019;92:e2109-17.